ATLAS Internal Note
CAL–NO–
RD3 note 59
August 8, 1994

Further Testbeam Results on the Electron Energy Resolution of the Barrel Accordion Calorimeter Prototype

Steven Robertson
and
Michel Lefebvre

University of Victoria, British Columbia, Canada

Abstract

The RD3 pointing accordion geometry barrel calorimeter prototype was recently tested at the CERN SPS using electron beams with energy 10 GeV to 287 GeV. Data taken in the spring and autumn of 1993 were analysed. The energy response of the calorimeter was found to vary with the electron impact point with an rms of $\sim 0.5\%$ in η and ϕ. After applying position dependent response corrections and optimizing the energy weighting with respect to the longitudinal segmentation, an energy resolution of $(0.40 \pm 0.07)\% \oplus (10.2 \pm 0.6)\%/\sqrt{E} \oplus (0.33 \pm 0.02)/E$ (where E is in GeV) and a large scale response uniformity of $0.61\% \pm 0.05\%$ were obtained for this prototype at an average pseudorapidity of $\eta = 0.11$ with a readout time of ~ 35 ns.

1 Introduction

The barrel electromagnetic (EM) calorimeter of the ATLAS detector will use a liquid argon (LAr) sampling technique with a pointing accordion geometry and a fast readout scheme [1] which was developed by the RD3 collaboration [2, 3]. We report here on the analysis of electron data taken in the spring and autumn of 1993 on a large scale prototype of the EM barrel accordion calorimeter [4] constructed and tested by the RD3 collaboration. This note complements the comprehensive results previously reported [5] in that most of the data used here had not been analysed before. The energy resolution to electrons and the corrections used are described in section 2, followed by a result on large scale response variations.

Description of the prototype, the performance of the readout chain and the experimental setup can be found in [4, 5].

2 Electron Energy Resolution

Data from secondary and tertiary electron beams from the spring and autumn of 1993 tests were analysed. Electron showers were reconstructed as in [5] (except that a 3×3 cluster was used in the back sampling in this analysis as opposed to a 3×2 cluster), yielding electron samples of energy 10, 20, 30, 197.5 and 287 GeV. Only results from sector 1 ($0 < \eta < 0.21$) are presented unless otherwise specified.

2.1 Uncorrected energy resolution

The width and the mean of the electron energy peak were determined by performing a Gaussian fit to the region surrounding the peak but excluding the non-Gaussian low energy tail (see [5]). A contribution to the width of 0.7% (0.3% for $E > 30$ GeV) due to the beam momentum spread [3] was quadratically unfolded from σ/μ to give the uncorrected energy resolution of the calorimeter. The uncorrected resolution was determined at each available electron beam energy using data from the Si sector 1 region [5]. At 10, 20 and 30 GeV the uncorrected resolution was measured using $\sim$ 3 runs at each energy taken in a single cell. Data from several different cells were combined in order to obtain average values for the resolution at 197.5 GeV and 287 GeV. To isolate the intrinsic energy resolution performance, response variations between cells were eliminated by individually normalizing the mean response in each cell to one (see also section 3). This was verified by comparing the average value of the resolutions obtained for the individual runs with the resolution obtained when all of the individually normalized runs were combined. The two values were found to be the same within statistical errors. The uncorrected energy resolution is plotted as a function of the incident beam energy in figure 1. A fit yielded the expression

$$\frac{\sigma(E)}{E} = (0.82 \pm 0.04)\% \oplus \frac{(11.4 \pm 0.7)\%}{\sqrt{E}} \oplus \frac{0.30 \pm 0.03}{E} \quad , \qquad (1)$$

where E is in GeV.

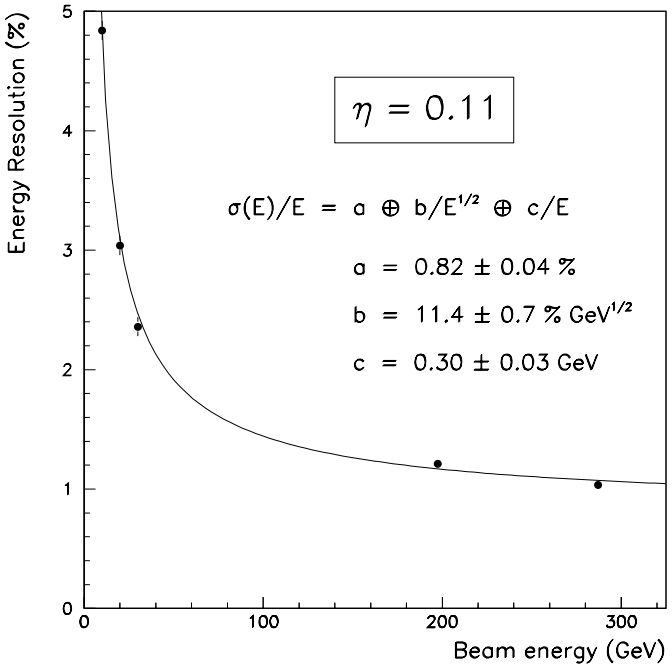

Figure 1: Uncorrected energy resolution as a function of the electron beam energy. Uncertainties in the data points are shown, or are smaller than the dots. The solid line represents the best fit to the data points and the values of the parameters a, b and c are listed. E is in GeV.

2.2 Sampling weighting corrections

Segmentation of the calorimeter in depth permitted the shower to be sampled at three different depths longitudinally. The total energy of the shower was reconstructed by a weighted sum of the energy measured by a 3×3 cluster of cells in each sampling. The general form of the weighted sum used is

$$E = \alpha(E_1 + \beta(E_2 + \gamma E_3)) \qquad , \tag{2}$$

where E is the reconstructed shower energy, E_i is the energy measured in the i_{th} sampling, and α, β, γ are weighting factors. In this parameterization β and γ are free parameters and α is chosen so that the mean value of E is equal to the mean energy of the uncorrected samples as described in section 2.1. Because the energy resolution is given by the ratio of the peak width to the mean energy, it is independent of the value of α.

There are several physical reasons why β and γ are not necessarily equal to unity. Charge deposited in the first sampling is transferred to preamplifers at the front face of the calorimeter, while signals from the second and third samplings are read out from the back. Narrow copper lines carry the signal from the middle sampling to the rear surface of the calorimeter. A small fraction of the ionization charge produced in the third sampling will

therefore be collected on these lines and contribute to the signal in the second sampling. The proximity of these lines to the electrodes is also known to produce crosstalk between the second and third samplings [5]. (Note that cell by cell crosstalk corrections were not applied here, unlike in [5]). Furthermore, the pointing accordion geometry causes a small variation with depth of the sampling frequency and of the electric field configuration near bends in the plates. Because the longitudinal shower profile is dependent on the incident particle energy, the parameters of equation 2 may also be energy dependent.

The resolution was optimized with respect to the parameters β and γ by fitting Gaussian functions to the energy distributions which were reconstructed using equation 2. The energy resolution was expected to be more sensitive to the value of β than to γ because a larger fraction of the total energy was deposited in the second sampling than in the third. Furthermore, β was presumed to have a value close to unity and to be less dependent on the beam energy. For these reasons an energy independent value for β was sought. The obvious choice $\beta = 1.0$ did not produce the best possible resolution at low energies, however $\beta = 0.93$ was found to be consistent with the optimum resolution at all available energies.

The optimum value for γ was estimated at each available beam energy by plotting the energy resolution as a function of γ with β fixed to 0.93. This is illustrated in figure 2 for 197.5 GeV electrons. The uncertainty in γ was taken to be the estimated variation in γ which degraded the resolution by an amount equal to the average uncertainty in the resolution.

At energies above 10 GeV γ was found to be consistent with 1.0, while at 10 GeV it was consistent with zero, as is shown in figure 3a. This can be understood by noting that the mean energy measured in the third sampling at this beam energy is only slightly above the level at which noise contributes to the signal. The electronics noise in cells equipped with Si MESFETs had previously be found to produce incoherent noise at the level of ~ 50 MeV in the first and second samplings, and ~ 70 MeV in the third sampling [5]. The total incoherent noise in the third sampling was therefore expected to be ~ 210 MeV, given by the quadratic sum of the noise in the nine cells in the energy cluster. The mean energy measured in the third sampling is plotted as a function of the beam energy in figure 3b, where the error bars indicate the rms of energy distribution. From this figure it is clear that electronics noise is the dominant contribution to the measured signal, and so setting γ to zero at low energies can improve the energy resolution.

The reconstructed energy was then conveniently parameterized by

$$E = \alpha(E_1 + 0.93 \cdot (E_2 + \gamma E_3)) \quad \text{where} \quad \gamma = \begin{cases} 0 & \text{if } E \leq 10 \text{ GeV} \\ 1 & \text{if } E > 10 \text{ GeV} \end{cases} . \tag{3}$$

The term *reconstructed energy* will be used from here on to refer to the weighted sum of a 3×3 energy cluster in each sampling computed using equation 3. The energy resolutions obtained at each beam energy using the reconstructed energies and yielded the results listed in table 1. The sampling and constant terms are seen to improve relative to the uncorrected resolution measured in section 2.1.

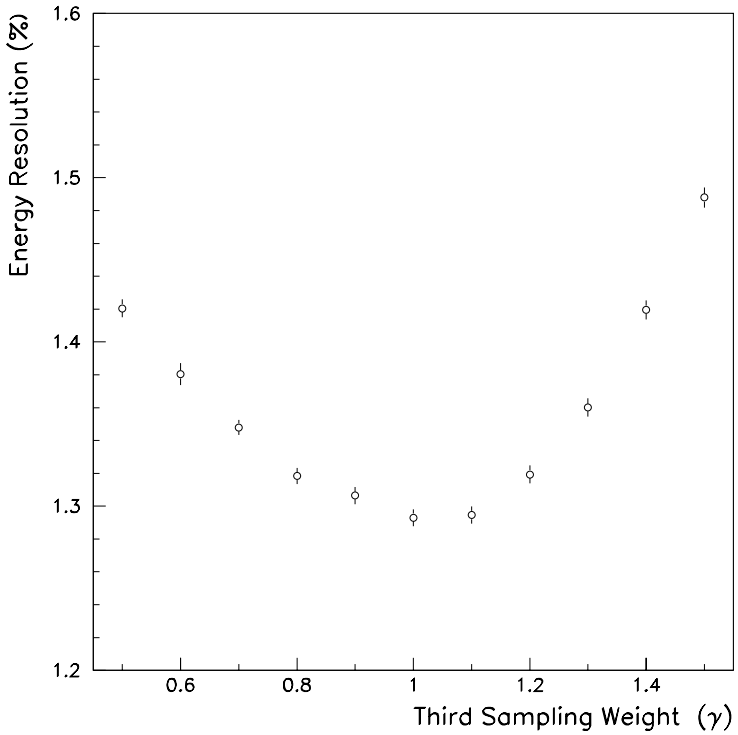

Figure 2: Energy resolution as a function of the third sampling weight γ for 197.5 GeV electrons in sector 1. The value of β was fixed to 0.93.

2.3 Position dependent corrections

2.3.1 Impact point reconstruction

Two independent methods were available for determining particle impact positions on the calorimeter face. Electron impact positions could be found by extrapolating the positions measured by the three wire chambers to the front face of the calorimeter [5]. Positions reconstructed in this way are referred to as *beam chamber positions*. This system required an accurate knowledge of the location of the cryostat, of the prototype within the cryostat and of the wire chambers in order to correctly map impact points onto the calorimeter face. Effects such as material shrinkage at cryogenic temperatures contribute to the uncertainty in these positions. As a result, the locations of cell edges and the exact size of calorimeter cells were not precisely known with respect to this coordinate system. These had to be determined by examining the calorimeter response to electron events (see section 2.3.2), introducing additional uncertainty to the beam chamber position measurements.

Cluster positions were determined by computing the energy weighted barycentre of a 3×3 cluster of cells in the first sampling of the calorimeter. Clustering effects tended to reconstruct impact points away from the cell edges in both η and ϕ, producing a small

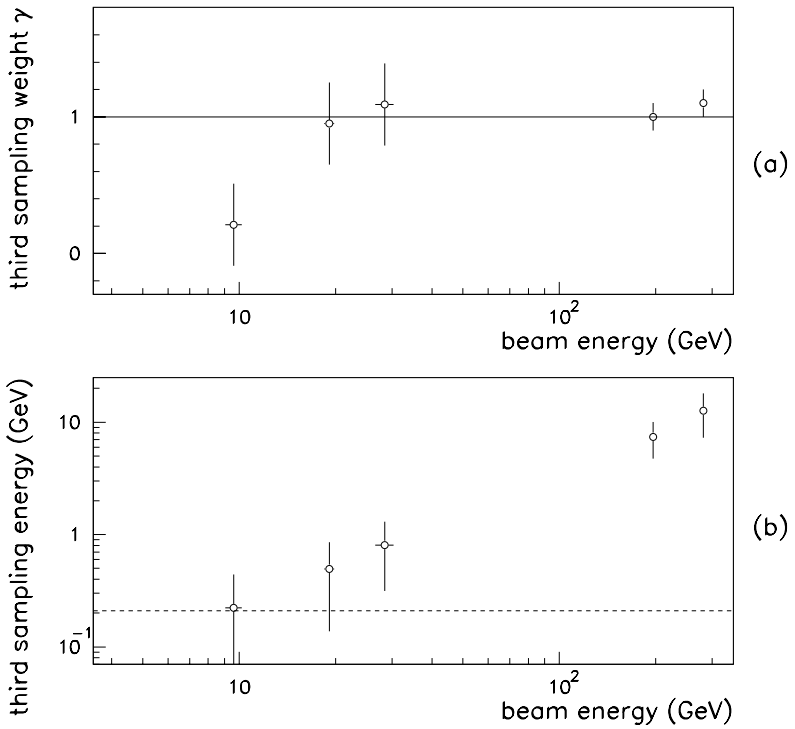

Figure 3: a) Estimated optimum value of the third sampling weight γ as a function of the particle energy. b) Energy deposited in the third sampling as a function of the reconstructed particle energy. The dashed line represents the rms of the electronics noise in the third sampling.

gap in the position spectrum at cell edges. The η cluster position consistently biased reconstructed impact points towards the centre of the cell, resulting in a well-known S-shaped curve when plotted against the beam chamber position, while the cluster position in the ϕ direction was linear with respect to the beam chamber position [3]. The η and ϕ positions are expressed in *cell units* in which the cell size is normalized to one and the cell centres are at integer values. Because calorimeter reconstructed cluster positions were directly tied to the calorimeter, they were not susceptible to the imperfections of the beam chamber position reconstruction. The size of the calorimeter cells and the location of cell edges were known precisely with respect to the cluster position coordinate system.

Comparisons between the beam chamber positions and the cluster positions reconstructed for different data runs indicated that there were systematic offsets in the beam chamber positions between runs. These were attributed to the encoders which provided the location of the cryostat. Plots of the calorimeter energy response as a function of the beam chamber η position (see section 2.3.2) were found to have a smaller rms than similar plots using cluster positions. This was attributed to the fact that the decrease

	$a(\%)$	b (% GeV $^{1/2}$)	c (GeV)
uncorrected	0.82 ± 0.04	11.4 ± 0.7	0.30 ± 0.03
cluster weighted	0.66 ± 0.05	10.5 ± 0.7	0.31 ± 0.03

Table 1: Comparison of the energy resolution fitting parameters a, b and c obtained with and without applying sampling weighting corrections to the electron data samples.

of the response near the cell edges was partially washed out by the uncertainty in the beam chamber position. Because the cluster position tends to bias impact points towards the cell centre, the position scale near the cell edges is effectively stretched so that the position resolution improves near the cell edges. This is due to increased energy sharing between cells in the nonet when an electron strikes the calorimeter near cell edges [6]. Position dependent energy corrections (section 2.3.3) were found to be more effective at improving the calorimeter energy resolution when cluster positions were used. Therefore, only cluster positions were retained.

2.3.2 Position dependent response variations

The position dependence of the energy response was determined by plotting the average reconstructed energy as a function of the impact point in η and ϕ as given by the cluster position. Because the amplitude of the position dependent response was somewhat smaller than the energy resolution of the calorimeter, it was necessary to combine electron data from runs in several different cells in order to obtain sufficiently good statistics to determine the shape of the η and ϕ response with a reasonable degree of precision. Approximately 50 000 events distributed over eighteen different cells in the Si sector 1 region were used to determine the calorimeter response to 197.5 GeV electrons. At 287 GeV, about 20 000 events in ten cells in the same region were used. The energy response of the accordion calorimeter was found to be dependent on the impact position of the incident particle within a cell at the $\sim$ 1% level in both the η and ϕ directions. The normalized calorimeter response to high energy electrons is plotted as a function of the η and ϕ positions in figure 4.

In the η direction the accordion calorimeter is geometrically equivalent to a parallel plate calorimeter, so the variation in the response is not due to geometrical effects, but to the clustering used to reconstruct the particle energy. A particle striking the calorimeter near the centre of a cell deposits most of its energy within a 3×3 cluster of cells surrounding the hit cell. The shower produced by a particle striking near the edge of a cell is not as well contained within this cluster and so the calorimeter response will decrease near cell edges. The response variation caused by this effect was measured using 197.5 GeV electron data to have an rms of $(0.69 \pm 0.03 \pm 0.01)\%$ (see table 2). This effect could be reduced by reconstructing the shower energy using 5×5 clusters of cells in order to reduce the energy leakage, however 3×3 energy clusters are preferable because they introduce less electronics noise. We note that other cluster sizes might be favoured by ATLAS.

The response variation in the ϕ direction is a combination of the clustering effect

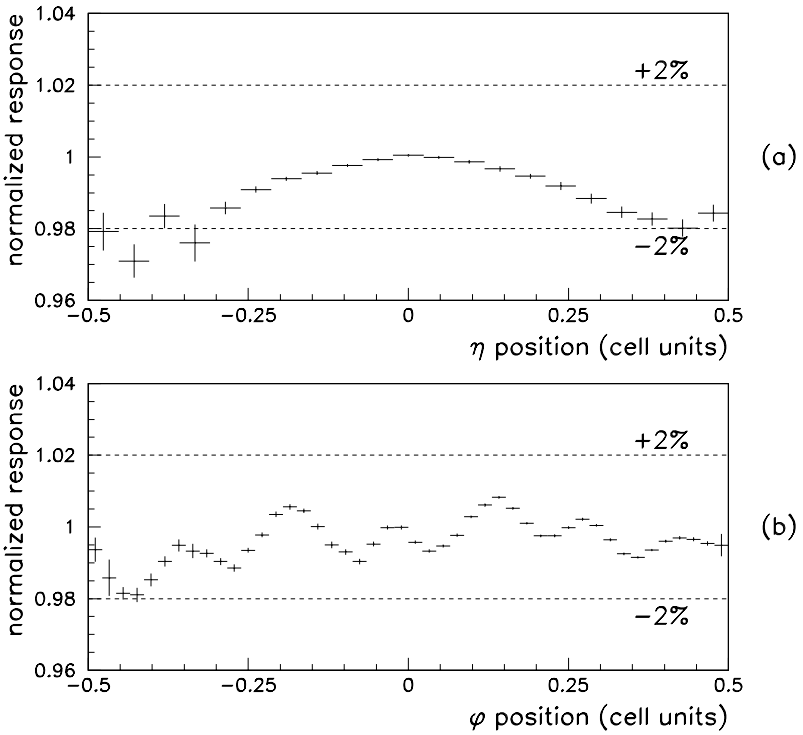

Figure 4: Normalized calorimeter response as a function of the electron impact point in η (a) and in ϕ (b). The statistical error on the average response in each bin is shown.

discussed above and geometrical effects related to the accordion structure. The origin of the geometrical effects can be understood by considering a hypothetical non-interacting particle passing though the calorimeter. The thickness of LAr traversed by such a particle varies with an rms of $\sim 2\%$ depending on the impact point within a cell [7]. This effect is reduced in the case of real particles by the transverse spread of the EM shower. However, the calorimeter response is enhanced when a particle is incident in a region of a cell where the average thickness of LAr traversed by particles in the shower is more than the average thickness over the entire cell. The three-fold structure resulting from the ganging of readout layers to form a readout cell is reproduced by the ϕ response. The rms of the response modulation in ϕ was measured using 197.5 GeV electrons to be $(0.61 \pm 0.03 \pm 0.05)\%$ and was approximately energy independent.

2.3.3 Response corrections

Position dependent response non-uniformities contribute directly to the constant term of the calorimeter energy resolution. It is therefore desirable to correct these effects to the highest degree that is practical, particularily at high energies where the constant term dominates. In the work described here, position dependent corrections were applied

to 197.5 GeV and 287 GeV electron data only, because at lower beam energies they were found to have no significant effect on the calorimeter energy resolution. Position dependent corrections can be applied either globally, in which case the same correction is applied to all cells in the calorimeter, or locally, where each cell is individually corrected with cell specific corrections. Because local corrections require high statistics in each cell, their effectiveness is difficult to evaluate. Only global corrections are retained in this work.

The procedure for applying and evaluating the effectiveness of position dependent corrections is as follows. The response was plotted as a function of each of the two coordinates η and ϕ as measured by the cluster position. The response variations with respect to the two coordinates are independent, so the mean energy response $R(\phi, \eta)$ is separable into functions of η and ϕ (see for example figure 4):

$$R(\eta, \phi) = F(\phi)\ G(\eta)\ . \tag{4}$$

These curves were then fitted with the functions $f(\phi)$ and $g(\eta)$, which approximated the true response $F(\phi)$ and $G(\eta)$. The electron data samples were then corrected on an event by event basis by dividing the reconstructed energy of each event by the normalized response function $r(\phi, \eta) = f(\phi)g(\eta)$. Because the function $r(\phi, \eta)$ is an approximation to the true response $R(\phi, \eta)$ there will in general be some residual position dependence.

The effectiveness of the position corrections was evaluated by comparing the energy resolution of the electron samples before and after corrections were applied. This gave a direct measure of the improvement resulting from the correction, however it only describes the true resolution of the calorimeter if the electron samples were uniformly distributed over each cell, which was not the case. The rms of the residual corrected response variation gives an indirect measure of the improvement in the resolution which is less subject to biasing. The corrected response was plotted as a function of each of the two position coordinates and the rms of the residual modulation was evaluated over one cell. The improvement in the resolution that can be expected by applying these corrections to a data sample uniformly distributed over a cell is given by the quadratic sum of the difference in the uncorrected and corrected rms values in η and ϕ. Poor statistics near cell edges increase the uncertainty of these measurements but do not bias the result. The values of the rms of the position dependent response variation and their residuals after correction are listed in table 2.

Systematic uncertainties in the position dependent response were estimated by comparing the cell to cell variations in the measured position dependent response before and after position dependent corrections were applied. The 197.5 GeV electron data sample was divided into two statistically independent samples on a cell by cell basis. Each sample was separately used to determine the response variation in η and ϕ. The systematic error in the rms of the position dependent response was determined by comparing the response curves for the two data samples. The η dependent response variation was found to show very little sensitivity to cell to cell response variations. This was to be expected since the η dependence of the response was attributed to clustering effects, and not to the mechanical structure of the calorimeter. The systematic error in the measurement of the η dependent response was estimated to be on the order of 0.01% and was attributed mainly to possible calibration errors in cells in the (3×3) energy clusters. The cell to cell variation in the

	rms (%)	Corrected rms (%)
η response at 197.5 GeV	$0.69 \pm 0.03 \pm 0.01$	$0.31 \pm 0.04 \pm 0.01$
η response at 287 GeV	$0.83 \pm 0.07 \pm 0.01$	$0.35 \pm 0.09 \pm 0.01$
Energy specific correction	–	$0.35 \pm 0.09 \pm 0.01$
ϕ response at 197.5 GeV	$0.61 \pm 0.03 \pm 0.05$	$0.21 \pm 0.4 \pm 0.05$
Corrected with $f_1(\phi)$	–	$0.43 \pm 0.3 \pm 0.05$
ϕ response at 287 GeV	$0.50 \pm 0.2 \pm 0.05$	$0.30 \pm 0.2 \pm 0.05$
Energy specific correction	–	$0.17 \pm 0.03 \pm 0.05$

Table 2: Values of the rms of the response variation in η and ϕ before and after position dependent corrections were applied. The statistical and systematic uncertainties are also listed. All corrections were made using $g(\eta)$ and $f_2(\phi)$ fitted to the response determined for the 197.5 GeV electron sample except where otherwise noted. "Energy specific corrections" utilize response functions which were fitted to data at 287 GeV.

ϕ dependent response was found to be much larger, possibly due to mechanical imperfections in the accordion structure of the cell. The uncertainty in the rms due to these effects was estimated to be 0.05%, and does not include differences in the response due to variations in the experimental setup between the two testbeam periods, such as possible slight differences between angles of incidence of the electron beam on the calorimeter face. Because the 197.5 GeV and 287 GeV electron samples were collected during two different testbeam periods, it is likely that the difference between the values of the rms of the ϕ dependent response measured at these two energies is entirely attributable to systematic effects rather than to an energy dependence of the response variation.

The normalized response in the η direction was fitted with the function

$$g(\eta) = P_1 + P_2 \sin(\pi\eta + \pi/2) \quad , \tag{5}$$

where η is in cell units and P_1 and P_2 are the fitting parameters. Figure 5 shows the η dependence of the response before and after applying this correction to 197.5 GeV data. The residual rms of $(0.31 \pm 0.04 \pm 0.1)\%$ was attributed to imperfections in the fit at the cell edges, and to the anomally at $\eta \approx 0.1$ which was a consequence of the beam profile at this energy. η corrections applied to 287 GeV data were also found to correct the rms to the $\sim 0.3\%$ level independent of whether the fitting parameters were obtained using 197.5 GeV data or 287 GeV data (see table 2). The residual rms was largely attributable to statistical variations in the response, due to low event statistics in some regions of the cell. The effectiveness of this simple correction at reducing the rms of the η dependence of the response, independent of the beam energy and testbeam setup, combined with the small value of the cell to cell variation in the η dependence, suggest that the it should be possible to correct the η dependent response to a high degree in an experiment such as ATLAS. In the present case, measurements of the effectiveness of η corrections are statistically limited. A uniform beam profile over an area of at least an entire cell during data taking would allow a more precise determination of the η dependent response.

Two different functions were used to fit the response in the ϕ direction. Initially

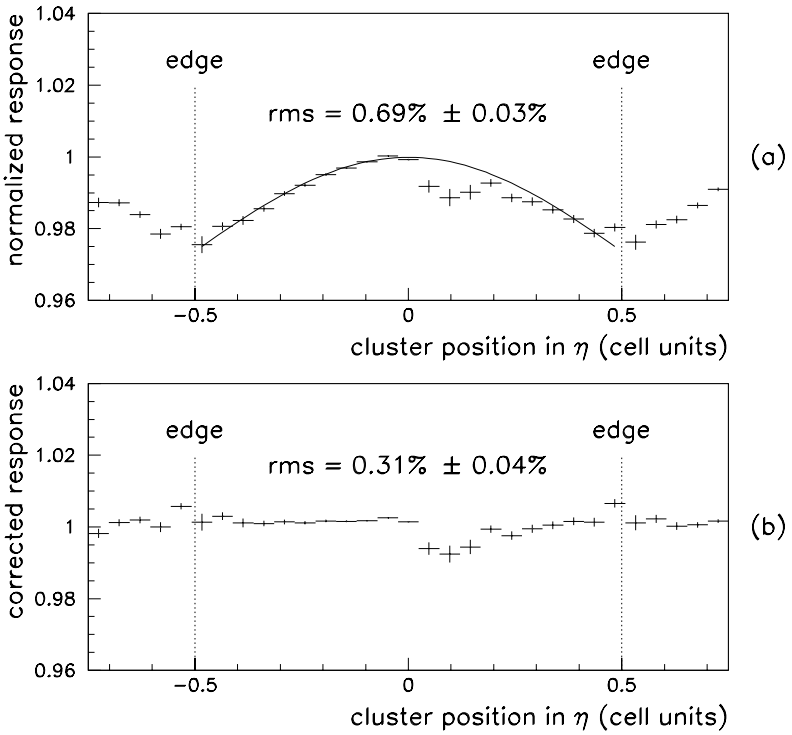

Figure 5: (a) The normalized response variation for 197.5 GeV electrons in η fitted with a correction function. (b) The response in η after the correction is applied.

a simple three parameter response function was used. This function was similar to that used in [5]:

$$f_1(\phi) = 1.0 + P_1\phi^2 + P_2\sin(6\pi\phi - \pi/2) + P_3\sin(12\pi\phi + \pi) \quad . \tag{6}$$

The decrease in response near cell edges due to the clustering effect is corrected by the quadratic term, and the remaining two terms describe the threefold structure of the calorimeter cells. This function was found to reproduce the basic shape of the ϕ response, but did not describe the response well. Corrections applied to 197.5 GeV electron data produced a residual ϕ dependence with an rms of $(0.43 \pm 0.04 \pm 0.05)\%$. This residual was largely attributable to the inadequacy of the response function rather than to statistical fluctuations, suggesting a need for a more specialized correction function. A second ϕ response correction function was obtained by using harmonics of $\sin(\pi\phi)$ and allowing the phases to vary freely. The resulting eight parameter function

$$f_2(\phi) = P_1 + P_2\sin(\pi\phi + \pi/2) + P_3\sin(2\pi\phi + P_4) + P_5\sin(6\pi\phi + P_6) + P_7\sin(13\pi\phi + P_8) \tag{7}$$

was found to describe the data very well. The first two terms correspond to the clustering effect, as for the η case. The last three terms correspond to effects due to the accordion

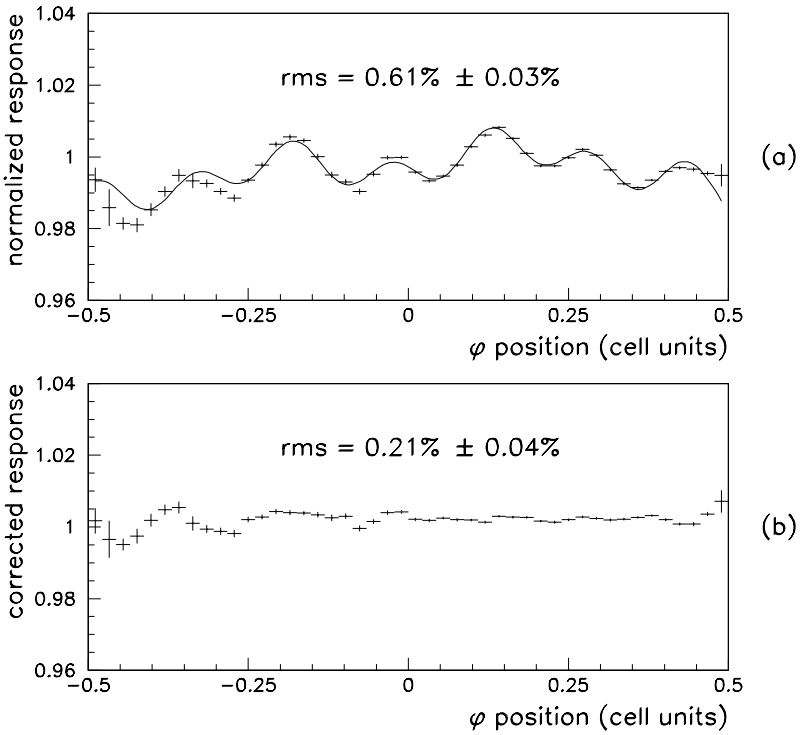

Figure 6: (a) The normalized response variation for 197.5 GeV electrons in ϕ fitted with an eight parameter correction function. (b) The response in ϕ after the correction is applied.

structure. The last term violates ϕ symmetry and is therefore not satisfactory; however a different term gave worse results. This effect is not yet understood. This function is shown in figure 6 fitted to the response curve obtained for 197.5 GeV electrons. The residual ϕ modulation after the correction was applied is also shown in this figure, and was found to have an rms of $(0.21 \pm 0.04 \pm 0.05)\%$. Comparison of the residual ϕ modulation obtained when 197.5 GeV and 287 GeV data were separately fitted with $f_2(\phi)$ indicates that this correction was equally effective at both energies. However, when the 287 GeV electron sample was corrected using the same function fitted to 197.5 GeV data, the residual rms was seen to worsen to $\sim 0.3\%$. This effect is probably due to differences in the calorimeter alignment between testbeam periods (see section 2.3.2) and cell to cell response variations, rather than indicating an energy dependence of the ϕ response. Reducing the rms of the residual response variation in ϕ direction to the level of $\sim 0.3\%$ has been shown to be relatively straightforward, however reducing it much beyond this level will clearly require more sophisticated corrections and a better understanding of systematics.

Beam Energy	10 GeV	20 GeV	30 GeV	197.5 GeV	287 GeV
Uncorrected	4.84 ± 0.05	3.04 ± 0.03	2.36 ± 0.04	1.21 ± 0.005	1.03 ± 0.01
Cell weighted	4.59 ± 0.05	2.93 ± 0.03	2.28 ± 0.04	0.998 ± 0.004	0.918 ± 0.008
Eta corrected	-	-	-	1.16 ± 0.004	0.994 ± 0.008
Phi corrected	-	-	-	1.07 ± 0.004	0.988 ± 0.008
All corrections	4.59 ± 0.05	2.93 ± 0.03	2.28 ± 0.04	0.808 ± 0.004	0.761 ± 0.008
Systematic error	± 0.07	± 0.07	± 0.07	± 0.02	± 0.02

Table 3: Measured electron energy resolution (in %) at various beam energies before and after corrections were applied (sector 1 electron samples). The estimated systematic and statistical errors are also listed.

2.4 Corrected energy resolution

The corrected electron energy resolution of the prototype was determined by applying sampling weighting and position dependent corrections to the electron samples. The resolution at 197.5 GeV and 287 GeV was determined by combining data from several cells. The mean reconstructed energy was normalized to one in each cell in order to correct for cell to cell response non-uniformities as discussed in section 2.1. Sampling weighting corrections were applied at all energies using the optimum weighting parameter values determined in section 2.2. Position dependent energy corrections were applied only to 197.5 GeV and 287 GeV electron data and used energy specific ϕ corrections. At lower energies where the resolution is dominated by electronics noise, position dependent corrections were found to have no significant effect and so were not used.

Systematic errors in the measured energy resolution were estimated in a manner similar to that used for the rms measurements (section 2.3.3). The 197.5 GeV electron sample was separated into two independent samples and the position dependence of the response was determined for each sample. The two samples were independently fitted with position dependent correction functions. The parameters obtained by fitting one sample with the functions $f_2(\phi)$ and $g(\eta)$ were used to correct the response of the other sample. The energy resolution obtained in this way was compared with the resolution measured when each sample was corrected using fitting functions determined on the same sample. The sensitivity of the energy resolution as to which data sample the response functions were originally fitted was found to be small. The cell to cell variation in the energy resolution was found to be significantly larger than the statistical uncertainty in the resolution measurements. The source of these variations in energy resolution was believed to be cell to cell variations in the ϕ dependence of the response as discussed previously. A systematic uncertainty of $\pm 0.02\%$ was estimated for the energy resolution measured at 197.5 GeV and 287 GeV. At lower energies where only a few data runs were available at each energy, the uncertainties were estimated using the variance of the measured resolutions.

The corrected energy resolutions are shown in table 3 and are plotted as a function of the beam energy in figure 7. It can be seen that each of the sampling weighting

	a(%)	b (% GeV $^{1/2}$)	c (GeV)
uncorrected	0.82 ± 0.04	11.4 ± 0.7	0.30 ± 0.03
corrected	0.40 ± 0.07	10.2 ± 0.6	0.33 ± 0.02
reference [5]	0.35 ± 0.04	9.99 ± 0.29	0.2823 ± 0.017

Table 4: Energy resolution fitting parameters obtained before and after η, ϕ and sampling weighting corrections were applied. The values reported by in [5], which were obtained using the same prototype but different data samples, are listed for comparison.

corrections, η corrections and ϕ corrections independently applied to the data samples produce an improvement in the energy resolution at all beam energies, and that the sampling weighting correction has the most significant effect. The energy dependence of the resolution was determined by a fit to the resolutions measured at the five available beam energies. Table 4 lists the values of the parameters a, b and c which were obtained for the uncorrected and corrected energy resolution. The results reported in [5] which were obtained for the same prototype during a different testbeam period are listed for comparison. The values of a, b and c determined during this analysis are consistent with these other measurements, in particular the values of c become practically identical if the different third sampling cluster sizes are taken into account.

3 Uniformity and Large Scale Response Variations

The energy resolution described in section 2.4 is the average resolution measured over a single cell of the calorimeter. Contributions from the cell to cell response variations due to calibration errors and fluctuations in the average response with time are not included in these results. These effects were corrected for in previous sections by normalizing the average energy in each cell to one on a run by run basis (see section 2.1). Cell to cell nonuniformities produce an additional contribution to the constant term describing the large scale energy resolution ($a_{\rm L}$) which is added in quadrature to the local constant term a:

$$a_{\rm L} = a \oplus a_{\rm C} \quad , \tag{8}$$

where $a_{\rm C}$ is the contribution from cell to cell response variations.

The large scale uniformity of the pointing geometry prototype was determined using 197.5 GeV electron data distributed over 30 cells in Si sectors 1 and 2 in the region not covered by the preshower. Three cells in this region with pathological behavior attributed to faulty preamplifiers were excluded. Sampling weighting and impact position corrections were applied to the data in the remaining 27 cells and the energy spectrum of the combined data was obtained. The large scale resolution was determined by fitting the energy response of this data sample with a Gaussian function in the region of the energy peak excluding the low energy tail. The local resolution was measured for the same data sample by applying a cell to cell normalization and measuring the width as before. The contribution to the resolution due to cell to cell response variations was then calculated by

quadratically unfolding the local energy resolution from the large scale resolution. These cell to cell response variations were found to contribute $(0.61 \pm 0.05)\%$ to the constant term of the resolution.

As a crosscheck to this measurement, the cell to cell response variation was estimated by computing the rms of the the distribution of mean energies measured in the 27 cells. This value was found to be $(0.64 \pm 0.05)\%$, which is in good agreement with the value obtained previously.

4 Conclusion

A large scale pointing accordion geometry LAr electromagnetic calorimeter prototype was constructed by the RD3 collaboration and tested at the CERN SPS in the spring and autumn of 1993 where it was exposed to electron beams ranging in energy from 10 GeV to 287 GeV.

The energy of electron events corresponding to an average pseudorapidity of $\eta = 0.11$ was reconstructed using a weighted sum of the energy deposited in a 3×3 cluster of cells in each of the three longitudinal compartments of the calorimeter. The values of the weighting parameters were adjusted to optimize the energy resolution at all available beam energies, resulting in

$$E \propto (E_1 + \beta(E_2 + \gamma E_3)) \qquad , \tag{9}$$

where E is the reconstructed shower energy, E_i is the energy measured in the i_{th} sampling, $\beta = 0.93$, $\gamma = 1.0$ for $E_{\rm beam} > 10$ GeV and $\gamma = 0.0$ for $E_{\rm beam} = 10$ GeV. The change in the weight of the rear compartment at low energies was justified on the basis of the electronics noise in this compartment.

The position dependence of the calorimeter energy response was found to have an rms of $(0.69 \pm 0.03)\%$ in the η direction and $(0.61 \pm 0.03)\%$ in the ϕ direction. In the η direction, this response was attributed to clustering effects and could be easily corrected by applying a position dependent correction. The ϕ dependent response was found to be more complicated due to the accordion structure of a readout cell. Position dependent corrections to the response in ϕ direction produced a residual position dependent response with an rms of $\sim 0.3\%$, and was limited by cell to cell variations in the ϕ dependent response. Improvements in the beam chamber positioning system and a more uniform distribution of electron events over the area of a readout cell in future tests would lead to further understanding of the position dependence of the response.

After sampling weighting and position dependent response corrections were applied, the local (over one cell) electron energy resolution was found to be described by

$$\frac{\sigma(E)}{E} = (0.40 \pm 0.07)\% \oplus \frac{(10.2 \pm 0.6)\%}{\sqrt{E}} \oplus \frac{0.33 \pm 0.02}{E} \qquad , \tag{10}$$

where E is in GeV. Cell to cell response variations were found to contribute $(0.61 \pm 0.05)\%$ to the local energy resolution yielding a large scale constant term of $(0.73 \pm 0.06)\%$. These values, obtained with a ~ 35 ns readout time, were shown to be consistent with other results reported for this prototype [5], and compare favourably with the ATLAS requirements of $1.0\% \oplus 10.0\%/\sqrt{E}$.

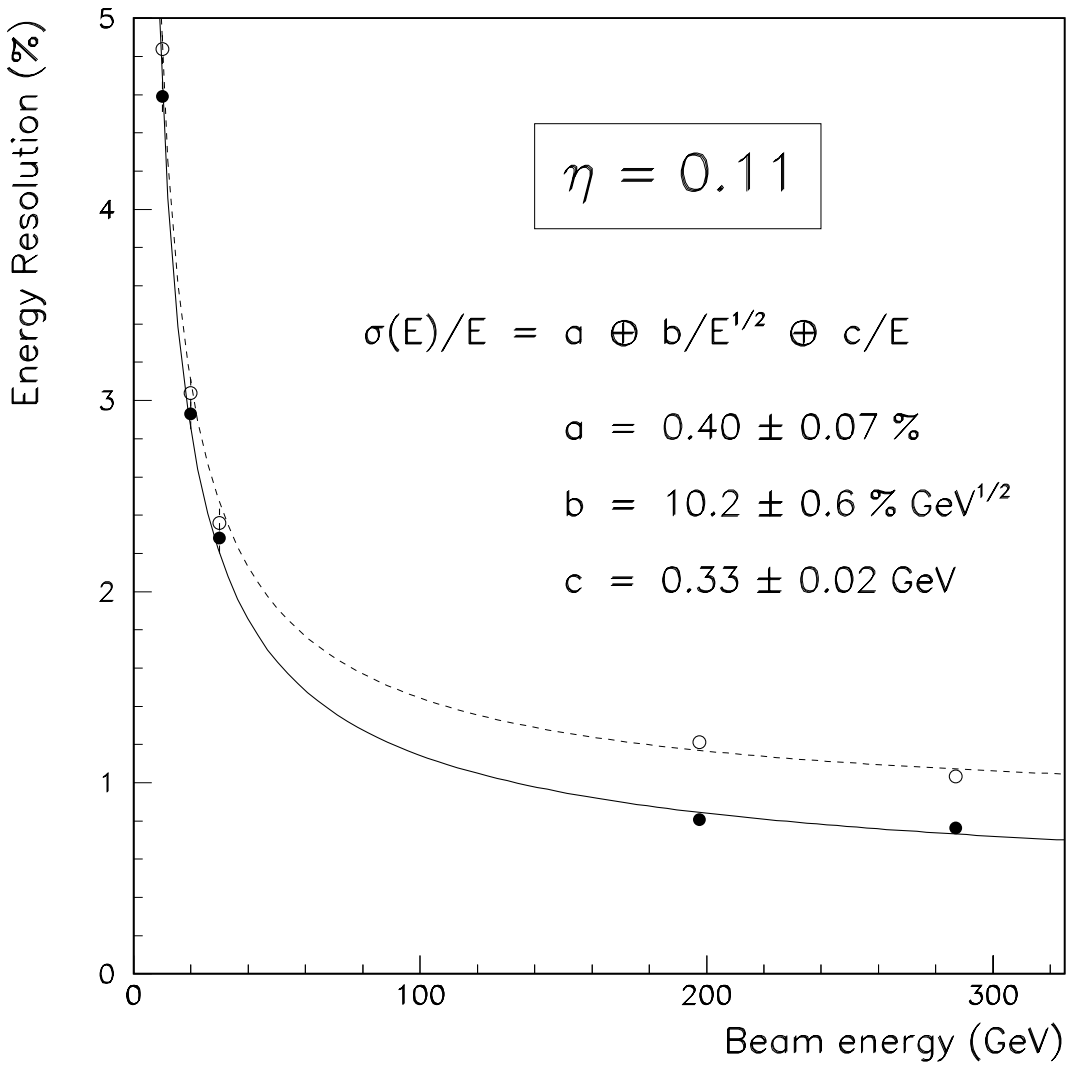

Figure 7: The electron energy resolution of the pointing geometry prototype for an average η of 0.11. The measured values of the uncorrected (open circles) and corrected (closed circles) resolution are plotted for the available beam energies. The dashed curve is the best fit to the uncorrected energy resolution, while the solid curve describes the resolution after all correction have been applied. The values of a, b and c obtained for the corrected energy resolution are listed.

References

[1] ATLAS Collaboration, *Progress Report on ATLAS Milestones*, CERN/LHCC/93-51, 15 October 1993.

[2] The RD3 collaboration has submitted the following DRDC documents:
Liquid Argon Calorimetry with LHC-Performance Specifications, CERN/DRDC/90-31, DRDC/P5, August 1990.
Hadronic and Electromagnetic Liquid Argon LHC Prototype Calorimeter with Pointing Geometry, CERN/DRDC/91-21, DRDC/P5-Add.1, March 1991.
R&D for a Liquid Argon Preshower, CERN/DRDC/92-40, DRDC/P5-Add.2, August 1992.
Status Report and Further R&D for EM and Hadronic Calorimetry, CERN/DRDC/93-4, January 1993.
RD3 Status Report, CERN/DRDC/94-18, 1994.

[3] The RD3 has the following published papers:
B. Aubert *et al.* (RD3 Collaboration), *Performance of a liquid argon electromagnetic calorimeter with an "accordion" geometry*, Nucl. Instrum. Methods **A309** (1991) 438-449.
B. Aubert *et al.* (RD3 Collaboration), *Performance of a liquid argon accordion calorimeter with fast readout*, Nucl. Instrum. Methods **A321** (1992) 467-478.
B.Aubert *et al.* (RD3 Collaboration), *Performance of a liquid argon electromagnetic calorimeter with a cylindrical accordion geometry*, Nucl. Instrum. Methods **A325** (1993) 116-128.
B. Aubert *et al.* (RD3 Collaboration), *Performance of a Liquid Argon Preshower Detector Integrated with an Accordion Calorimeter*, Nucl. Instrum. Methods **A330** (1993), 405-415.
D.M. Gingrich *et al.* (RD3 Collaboration), *Performance of a Liquid Argon Accordion Hadronic Calorimeter Prototype*, submitted to Nucl. Instr. Meth.

[4] D.M. Gingrich *et al.* (RD3 Collaboration), *Performance of a Large Scale Prototype of the ATLAS Accordion Electromagnetic Calorimeter*, paper in preparation.

[5] Andrea Cravero and Fabiola Gianotti, *Uniformity of response and energy resolution of a large scale prototype of the Barrel Accordion calorimeter*, ATLAS Internal Note, CAL-NO-33, RD3 Note 54, 11 April 1994.

[6] J.S. White, *Spatial Reconstruction of Electrons with an Accordion Geometry Electromagnetic Calorimeter*, Masters thesis, University of Victoria, 1993.
John White and Michel Lefebvre, *Spatial Reconstruction of Electrons with an Accordion Geometry Electromagnetic Calorimeter*, RD3 note 52, 10 January 1994.

[7] M. Lefebvre, G. Parrour and P. Pétroff, *Electromagnetic Liguid Argon Accordion Calorimeter Simulation*, RD3 note 41, 28 January 1993.

[8] ATLAS Collaboration, *Letter of Intent*, CERN/LHCC/92-4, 1 October 1992.